Partition function of the Potts model on self-similar lattices as a dynamical system and multiple transitions

Pedro D. Alvarez[1]*, Fabrizio Canfora[1]†, Luca Parisi[2]‡

[1] *Centro de Estudios Científicos (CECS), Valdivia, Chile*

[2] *Dipartimento di Fisica "E.R.Caianiello", Università di Salerno, I-84081 Baronissi (Sa), Italy*

INFN, Sezione di Napoli, GC di Salerno, I-84081 Baronissi (Sa), Italy

December 7, 2010

Abstract

We present an analytic study of the Potts model partition function on two different types of self-similar lattices of triangular shape with non integer Hausdorff dimension. Both types of lattices analyzed here are interesting examples of non-trivial thermodynamics in less than two dimensions. First, the Sierpinski gasket is considered. It is shown that, by introducing suitable geometric coefficients, it is possible to reduce the computation of the partition function to a dynamical system, whose variables are directly connected to (the arising of) frustration on macroscopic scales, and to determine the possible phases of the system. The same method is then used to analyse the Hanoi graph. Again, dynamical system theory provides a very elegant way to determine the phase diagram of the system. Then, exploiting the analysis of the basins of attractions of the corresponding dynamical systems, we construct various examples of self-similar lattices with more than one critical temperature. These multiple critical temperatures correspond to crossing phases with different degrees of frustration.

Keyword: Potts Model, dichromatic polynomial, Dynamical systems, fractals.

PACS: 12.40.Nn,11.55.Jy, 05.20.-y, 05.70.Fh.

Introduction

In the analysis of critical phenomena and phase transitions the dimensionality of the lattice plays a key role (see, for a detailed review, the classic book [1]). For instance, it is known that in the case of the Ising model on one-dimensional lattices without an external magnetic field the thermodynamics is rather uninteresting and long range correlations are exponentially suppressed. In the case of two-dimensional lattice models many interesting phase transitions do indeed occur and many exact results are known (see, for example, the classic review [2]). The intriguing geometry of fractals, whose (Hausdorff) dimension is generically a non-integer number, allows one to explore the phase diagrams of lattices whose dimension lie between one and two as well.

Usually, fractals have simple and recursive definitions, they display a fine structure at arbitrarily small scales in a "self-similar" fashion. Fractals often appear in the analysis of dynamical systems [3, 4]. Here it will be shown that, in a sense, the converse is also true: namely, the computation of the partition function on a large class of fractal lattices can be reduced to the analysis of a dynamical system.

We will concentrate on the Potts model which is the most natural generalization of the Ising model. This model is able to describe both first and second order phase transitions (detailed reviews on its connections with other areas in physics and mathematics are [2] and [5, 6, 7, 8]) thus it is an extremely important task to develop new methods in order to provide one with the exact phase diagram of the Potts model on interesting lattices. It is much harder to solve the Potts model for generic spin states number q rather than the Ising model: only the Ising model on a square lattice has been solved in the theormodynamical limit by Onsager [9] while the analytic solution of the Potts model in two dimensions on infinite square lattice is still to be found. Very few exact results of the Potts model are known in dimensions higher than one[1] (see [2]).

*alvarez AT cecs.cl

†canfora AT cecs.cl

‡parisi AT sa.infn.it

[1] Strip lattices i.e. periodic lattices whose length is much larger than their width, can provide interesting qualitative informations about the thermodynamics of the Potts model (see, for instance [10, 11, 12] and references therein). On the other hand, strip lattices are very close to be one-dimensional systems: in particular, their Hausdorff dimension is one.

The main goal of this paper is to use a technique which allows to apply the powerful tools of dynamical systems theory to study the Potts model on self similar lattices of fractal dimensions higher than one. We will focus on two special cases, the Sierpinski gasket and the Hanoi graph but the same ideas can be applied in more general cases.

The analysis of the Potts model on Sierpinski gasket has a long and interesting history began with the pioneering papers [13, 14, 15, 16, 17, 18]. In these papers, besides the intrinsic theoretical interest of a detailed analysis of the Potts model on self-similar lattices, it has been emphasized the importance of this analysis to shed more light on the theory of critical phenomena.

The papers [19, 20, 21, 22, 23, 24, 25, 26], have been important sources of inspiration as far as the present paper is concerned. In [19] the authors derived a discrete dynamical system to analyze the Potts model on the Bethe lattice. In [20], using ideas from the renormalization group techniques, the authors analyzed the partition function of a Potts model with an extra term in a magnetic field on a Sierpinski triangle: they derived and analyzed numerically exact algebraic relations among the system at the n-th and $(n+1)$-th steps of the recursive procedure. In [21, 22] the authors dealt with the same problem from the point of view of the renormalization group discussing the scheme (in)dependence of their results as well. In [23, 24, 25, 26] the authors derived exact recursion relations for the critical behaviors as well as the Fisher and Lee-Yang zeros of the Potts model on various hierarchical lattices: these recursion relations have been analyzed using dynamical system theory.

The key idea to analyse the partition function of the Potts model on self-similar lattices is to exploit in a direct way the corresponding recursive symmetry, according to the point of view of [27]. In these works, recursive symmetry has been used to get a phenomenological description of the Ising model in three dimensions in a quite good agreement with the available numerical data. In a recent paper [28], following the results presented in [29], it has been proposed to analyze strip lattice using the formalism of the dichromatic polynomial (a very well known tool in graph and knot theory: see, for instance [30, 31, 32]). One can determine a simple set of linear recursive equations whose solutions represent the sought partition function for strip lattices. In the present paper we will show that, using the dicrhomatic polynomial and introducing suitable geometrical coefficients, one can derive an exact discrete dynamical systems whose solution represents the sought partition function of the Potts model on self-similar lattices. The variables of this dynamical system have a clear physical interpretation in terms of (the arising of) macroscopic frustration and they allow to easily construct directly at each step the corresponding partition function. The study of this systems allows to determine the presence of a phase transition. Furthermore, this geometrical construction provides one with a clear physical interpretation of the possible changes of initial data.

The present formalism has three main advantages. First, the technique to derive the exact dynamical system can be very easily adapted to various self-similar lattices such as the Hanoi graph (which will be analysed here) and many others. Second, *the same dynamical system is able to describe a larger class of fractal lattices* with the same self-similar structure but different "initial conditions" as it will be explained in the next sections. The main advantage of the present approach is that it provides one with a very clean way to construct analytically systems with multiple transitions. This can be achieved by looking at the basins of attractions of the fixed points of the dynamical system corresponding to the self-similar lattice and then searching for suitable initial data which cross more than once the boundaries between different basins of attractions. To the best of the authors knowledge, this simple method to generate lattices with multiple transitions is new.

The paper is organized as follows: in section 1, the Sierpinski gasket is introduced along with its recursive definition and its fractal properties. In section 2, a recursive procedure to compute the partition function of the Potts model using the dichromatic polynomial is described. In section 3, an algorithm is outlined aimed to achieve a closed set of recursive equations by introducing suitable geometric coefficients related to the connectivity pattern of the vertices of the lattice. In section 4, a decomposition of the partition function for the Potts model at generic recursive step $n+1$ in terms of the partition function at step n is described. The procedure leads to a discrete dynamical system which completely characterize the relevant thermodynamical properties of the Potts model. In section 5, the same method is applied to the study of the Potts model on a different lattice, i.e. the Hanoi graph. In section 6, new sets of initial conditions for same dynamical system are considered. In section 7, the construction of self-similar lattices leading to multiple phase transitions is discussed. Some conclusions are eventually drawn.

1 The Sierpinski gasket

Let us consider the following recursive sequence of lattices which will be labelled as $T(n)$ where the label n denotes the recursive step (Fig.1).

The lattice $T(1)$ is nothing but a triangle. The lattice $T(2)$ can be obtained from $T(1)$ by adding three new vertices in the midpoints of the three edges of $T(1)$ and joining them by three new edges in such a way that the original triangle $T(1)$ is divided into four triangles and so on. Thus, the lattice $T(n+1)$ can be see as three lattices $T(n)$ joined in such a way that each of the three triangles $T(n)$ has just one vertex in common with each of the

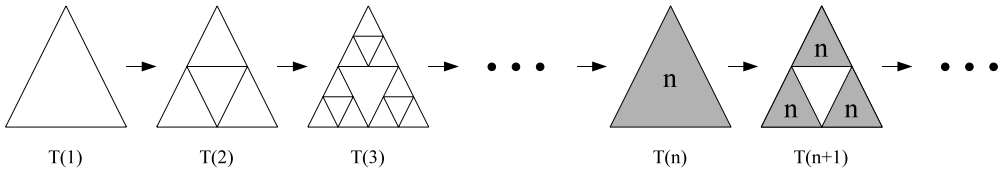

Figure 1: $T(1)$ is a lattice with three vertices and three edges, $T(2)$ is a lattice with six vertices and nine edges, $T(3)$ is a lattice with fifteen vertices and twentyseven edges and so on. In general, the number of vertices at step n is $(3^n+3)/2$ while the number of edges is 3^n. The number of internal sites of $T(n)$ is $(3^n-3)/2$ and the number of external sites is always 3.

other two $T(n)$ triangles. The $n \to \infty$ limit leads to the well known fractal structure named Sierpinski triangle or Sierpinski gasket.

The most interesting characteristic of this lattice is that, unlike the Bethe lattice, the $T(n)$ lattices (when n is very large) have many non-trivial closed paths. This is a very important characteristic since it is well known (see, for instance, [1]) that the absence of non-trivial closed paths on a lattice can make the corresponding partition function trivial. For this reason, the phase diagram of fractal lattices without a large enough number of loops (such as the Koch snowflake) would be uninteresting.

Indeed, for $n \to \infty$, $T(n)$ can be considered as a lattice living in more than one dimension, its Hausdorff dimension[2] d_H being

$$d_H = \frac{\log 3}{\log 2} \approx 1.585.$$

The only known lattices on which it is possible to find the exact partition functions of the Potts model are strip lattices of finite width. It is trivial to see that, for any finite width, the Hausdorff dimensions of these lattices is always one. Thus, even if strip lattices can often provide one with valuable informations on the thermodynamics of more realistic systems, it is clear that from the quantitative point of view they cannot go really beyond one dimensional physics. On the other hand, the class of $T(n)$ lattices defined above live naturally in more than one dimension and for this reason the corresponding thermodynamics could be very interesting.

2 Dichromatic Polynomial and the Partition function

The most useful way to compute the Potts model partition function for the purposes of the present paper is through the dichromatic polynomial (for a detailed review see [31]). This is a very powerful and pliant formalism suitable for a very wide range of application since it was designed to deal with generic types of lattices. The dichromatic polynomial $K[X]$ of a lattice X coincides with the partition function of the Potts model on X (see, for instance, [5]). It depends on the variable q, the number of spin states *per site*, and on the variable

$$v = \exp(\beta J) - 1, \tag{2.1}$$

where $\beta = 1/k_B T$, k_B is the Boltzmann's constant, T is the temperature and J is the coupling. It is also worth noting here that the ranges $-1 \leq v \leq 0$ and $0 \leq v \leq \infty$ correspond to the antiferromagnetic regime and the ferromagnetic regime respectively.

The dichromatic polynomial $K[X]$ of a graph X can be computed by a successive application of the following rules:

1. *(deletion-contraction algorithm)* the dichromatic polynomial of a graph X in which two points are connected by an edge $K[\bullet - \bullet]$ is equal to the sum of the dichromatic polynomial $K[\bullet\ \bullet]$ of a graph obtained from X by removing the edge plus v times the dichromatic polynomial $K[\bullet = \bullet]$ of a graph obtained from X by collapsing the edge [3] so that the external vertices of the edge are identified, i.e.

$$K[\bullet - \bullet] = K[\bullet\ \bullet] + v\ K[\bullet = \bullet], \tag{2.2}$$

[2]The Hausdorff dimension coincides with the usual definition of dimension in the case of regular lattices: for any regular two dimensional lattices in the thermodynamical limit $d_H = 2$, for regular three dimensional lattices $d_H = 3$ and so on.

[3]we will also use the terms "contracting" and "identifying".

2. the dichromatic polynomial $K\left[\bullet \cup X\right]$ of a graph X plus a point not connected with X, is equal to the product of the dichromatic polynomial of X times q, i.e.

$$K\left[\bullet \cup X\right] = q\, K\left[X\right], \tag{2.3}$$

3. the dichromatic polynomial of a single point is equal to q, i.e.

$$K\left[\bullet\right] = q. \tag{2.4}$$

As far as the goals of the present work are concerned, the most important property of the definitions in Eqs. (2.2), (2.3) and (2.4) is that they are *local* rules: namely, such rules act on an edge (or on a point) and they do not depend on the structure of the graph far from the edge (or the point) on which they are acting.

The basic idea of the present paper is to directly exploit the recursive symmetry of the class of lattices $T(n)$ in order to construct analytically the partition function of $T(n)$ which will be denoted as $K\left(n\right)$:

$$K\left(n\right) = K\left[T(n)\right],$$

and certainly the use of the rules 1, 2 and 3 is a key point to achieve that.

The geometry of self-similar lattices suggests to search for an inductive procedure which should allow one to construct the partition function at step $n+1$ from the informations of the step n. Thus, the question is, *which is the minimal amount of physical informations coming from the step n needed in order to construct* $K(n+1)$?

Using properly Eqs. (2.2), (2.3) and (2.4) and introducing suitable geometrical coefficients characterizing the connectivity patterns of the vertices of the Sierpinski gasket, it is possible to derive the exact expression of the partition function $K\left(n+1\right)$ at step $n+1$ in terms of the geometric coefficients of the step n. As it will be shown in the next sections, in this way one reduces the problem of computing $K(n)$ to the problem of analysing a simple dynamical system which lead to a quite clear analysis of the thermodynamical properties of $T(n)$ in the large n limit.

3 Connectivity coefficients of $T(n)$

In this section we will describe how the *connectivity coefficients* defined below appear as the natural set of variables to describe the phase diagram of the system. The lattices we are interested in have triangular shape and symmetry under $2\pi/3-$rotations: the three external vertices $\bullet_a$, $\bullet_b$ and $\bullet_c$ of $T(n)$ will be treated as marked points. Let us apply the rules of the dichromatic polynomial to every edge and to every internal vertex of the graph $T(n)$ *but without evaluating the three vertices*[4] $\bullet_a$, $\bullet_b$ and $\bullet_c$ of $T(n)$. Five different types of terms arise: in first place there are the terms where none of the marked points $\bullet_a$, $\bullet_b$ and $\bullet_c$ are identified. Secondly, there are the terms in which just two of the three marked points are actually identified (there are three possible pairs: $\bullet_a = \bullet_b$, or $\bullet_a = \bullet_c$, or $\bullet_b = \bullet_c$). The fifth possibility is that all the marked points $\bullet_a$, $\bullet_b$ and $\bullet_c$ are identified. Thus, one can express $K\left[T(n)\right]$ in the following way

$$K\left[T(n)\right] = x(n)K\left[\bullet_a\, \bullet_b\, \bullet_c\right] + y(n)\left(K\left[\bullet_a = \bullet_b\, \bullet_c\right] + K\left[\bullet_a = \bullet_c\, \bullet_b\right] + K\left[\bullet_a\, \bullet_b = \bullet_c\right]\right) + z(n)K\left[\bullet_a = \bullet_b = \bullet_c\right], \tag{3.1}$$

where the connectivity coefficients are $x(n)$, $y(n)$ and $z(n)$. So far, the expression (3.1) is a generic ansatz for any lattice with the same structure of external points $\bullet_a$, $\bullet_b$ and $\bullet_c$ and symmetry under $2\pi/3$-rotations. Of course, the partition function $K(n)$ and the connectivity coefficients satisfy the following relation

$$K\left(n\right) = q^3 x\left(n\right) + 3q^2 y\left(n\right) + qz(n)\ . \tag{3.2}$$

To clarify the above definitions, let us consider the simplest example: the partition function of $T(1)$. It is easy to check that the connectivity coefficients of the triangle $T(1)$ are

$$x(1) = 1, \qquad y(1) = v, \qquad z(1) = v^2\left(3+v\right), \tag{3.3}$$

thus replacing (3.3) in (3.1) and recalling that

$$K\left[\bullet_a\ \bullet_b\ \bullet_c\right] = q^3, \qquad K\left[\bullet_a = \bullet_b\, \bullet_c\right] = q^2 = K\left[\bullet_a\, \bullet_b = \bullet_c\right] = K\left[\bullet_a = \bullet_c\, \bullet_b\right], \qquad K\left[\bullet_a = \bullet_b = \bullet_c\right] = q, \tag{3.4}$$

one immediately recovers the usual expression for the partition function of $T(1)$.

[4]Namely, when the dichromatic polynomial $K[\,]$ acts on some of the three vertices $\bullet_a$, $\bullet_b$ and $\bullet_c$ we will not use the rule in Eq. (2.4).

The physical interpretation of the connectivity coefficients in terms of the phase diagram of the system is quite transparent (see Fig.2- Fig.6). When n is very large (which is the thermodynamical limit), one can classify the phases of the system as follows: the range of temperatures in which

$$\left|\frac{y\left(n\right)}{x\left(n\right)}\right| \underset{n\to\infty}{\ll} 1, \qquad \left|\frac{z\left(n\right)}{x\left(n\right)}\right| \underset{n\to\infty}{\ll} 1, \tag{3.5}$$

is a sort of a high temperature phase since, when the above inequalities hold, long range correlations are suppressed. This is clear from (3.1) because $x(n)$ is the coefficient which corresponds to the terms of $K(n)$ where the vertices $\bullet_a$, $\bullet_b$ and $\bullet_c$ of $T(n)$ are not identified. Hence, the coefficient $x(n)$ weighs the terms of $K(n)$ which correspond to spin configurations of $T(n)$ where the spins sitting at the vertices $\bullet_a$, $\bullet_b$ and $\bullet_c$ are not correlated.

On the other hand, if in the large n limit, one has

$$\left|\frac{y\left(n\right)}{x\left(n\right)}\right| \underset{n\to\infty}{\gtrapprox} 1, \qquad \left|\frac{z\left(n\right)}{x\left(n\right)}\right| \underset{n\to\infty}{\gtrapprox} 1, \tag{3.6}$$

then (at least) one pair of the external vertices are identified (for definiteness, let us take $\bullet_a$ and $\bullet_b$). By definition of $y\left(n\right)$ and $z\left(n\right)$, this implies that in this phase it appears (at least) one huge path (let us call this path $\gamma_{a\longleftrightarrow b}$) of neighbouring vertices which connects $\bullet_a$ and $\bullet_b$ such that all the spins sitting at the vertices of the path $\gamma_{a\longleftrightarrow b}$ are in the same state. This is particularly interesting in the antiferromagnetic phase $-1 \leq v \leq 0$ since, at low temperatures, the spin degrees of freedom sitting on neighbouring vertices "would like to be" in different states. If, at low enough temperatures, it is not possible to satisfy the constraint of having neighbouring spins in different states one says that *frustration* appears. Therefore, the present variables are very well suited to detect the arising of frustration at macroscopic scales since, in the large n limit, the number of spin degrees of freedom belonging to path $\gamma_{a\longleftrightarrow b}$ tends to infinity. The main goal of the present paper will be to establish if and when the Potts model on the Sierpinski gasket $T(n)$ (and, in the next sections, on the Hanoi graph) in the large n limit has only the high temperatures phase or if a "frustrated phase" appears as well. As it will be explained in the next section, one can answer this question quite elegantly by means of the analysis of the fixed points of a suitable dynamical system.

The next step is to exploit the self similarity of the Sierpinski gasket in order to derive a set of equations that relating the connectivity coefficients of the step $n+1$ to the ones of the step n. Indeed, one could compute directly by "brute force" the three geometric coefficients $x(n)$, $y(n)$ and $z(n)$: one should consider the Sierpinsky triangle after the $n-$th step and use the basic definitions in Eqs. (2.2), (2.3) and (2.4) without evaluating the three special points of $T(n)$. However, it is very easy to see that in this way the number of terms to compute grows faster than exponentially with the number of edges. The connectivity coefficients in Eq. (3.1) are defined in order to avoid a brute force computation as it will be shown in the next section.

4 Decomposing $K(n+1)$

In this section we will show how to express the partition function $K(n+1)$ of $T(n+1)$ and the coefficients $x(n+1)$, $y(n+1)$ and $z(n+1)$ at step $n+1$ in terms of the coefficients $x(n)$, $y(n)$ and $z(n)$ at step n. The vertices of $T(n+1)$ (which will be called $\bullet_A$, $\bullet_B$ and $\bullet_C$) will be the marked points. Each of the three $T(n)-$blocks composing $T(n+1)$ can be further decomposed into five terms according to Eq. (3.1). Then, one has to collect the terms which multiply $[\bullet_A \ \bullet_B \ \bullet_C]$ (they will form the coefficient $x(n+1)$), all the terms which multiply $[\bullet_A = \bullet_B \ \bullet_C]$ (they will form the coefficient $y(n+1)$) and all the terms which multiply $[\bullet_A = \bullet_B = \bullet_C]$ (they will form the coefficient $z(n+1)$). After this step, one simply needs to collect the terms which arise according to the connectivity patterns of the vertices $\bullet_A$, $\bullet_B$ and $\bullet_C$ of $T(n+1)$ (see Fig.2- Fig.6). The result of this operations is the following dynamical system:

$$x(n+1) = f(x(n), y(n), z(n); q), \qquad y(n+1) = g(x(n), y(n), z(n); q), \qquad z(n+1) = h(x(n), y(n), z(n); q), \tag{4.1}$$

with the initial data given by

$$x(1) = 1, \qquad y(1) = v, \qquad z(1) = v^2\left(3+v\right). \tag{4.2}$$

The functions f, g and h are homogeneous polynomials of degree 3 in the dynamical variables:

$$\begin{aligned} f(x,y,z;q) &= q^3x^3 + 9q^2x^2y + 3qx^2z + 24qxy^2 + 12xyz + (14+q)y^3 + 3y^2z, & (4.3)\\ g(x,y,z;q) &= 4qy^3 + q^2xy^2 + 7y^2z + 2qxyz + yz^2 + xz^2, & (4.4)\\ h(x,y,z;q) &= z^3 + 6yz^2 + 3qy^2z. & (4.5) \end{aligned}$$

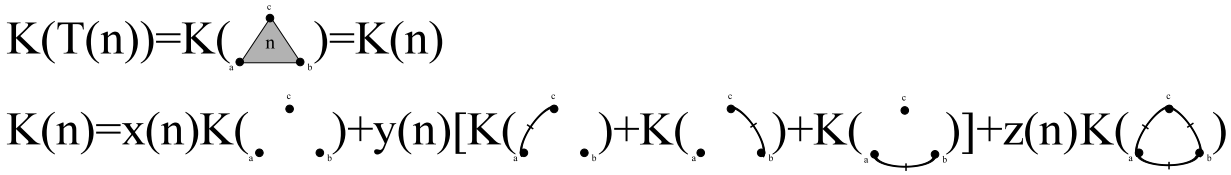

Figure 2: Decomposition of the partition function $K(n)$ corresponding to the lattice $T(n)$ according with the pattern of connectivity of its external vertices (denoted as $\bullet_a$, $\bullet_b$ and $\bullet_c$). Applying the defining rules of the dichromatic polynomial, i.e. Eqs. (2.2), (2.3) and (2.4), to $T(n)$ with the exception of the external vertices $\bullet_a$, $\bullet_b$ and $\bullet_c$, three types of terms arise. The first type of terms corresponds to the case in which three is no contraction between the external vertices. The second type of terms corresponds to the case in which two of the three vertices are contracted. The third type of terms corresponds to the case in which all the three external vertices are contracted. The contribution of the three types of terms to $K(n)$ will be denoted as $x(n)$, $y(n)$ and $z(n)$ respectively.

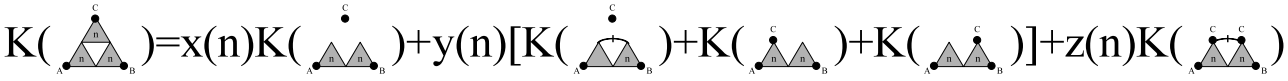

Figure 3: Decomposition of the partition function $K(n+1)$ at step $n+1$ using the definition of the geometric coefficients $x(n)$, $y(n)$ and $z(n)$ at step n according to the connectivity patterns of the external vertices. The three blocks constituting $T(n+1)$ have to be decomposed keeping track of the connectivity of each block. From the first block one gets five terms, each one of them has to be further decomposed.

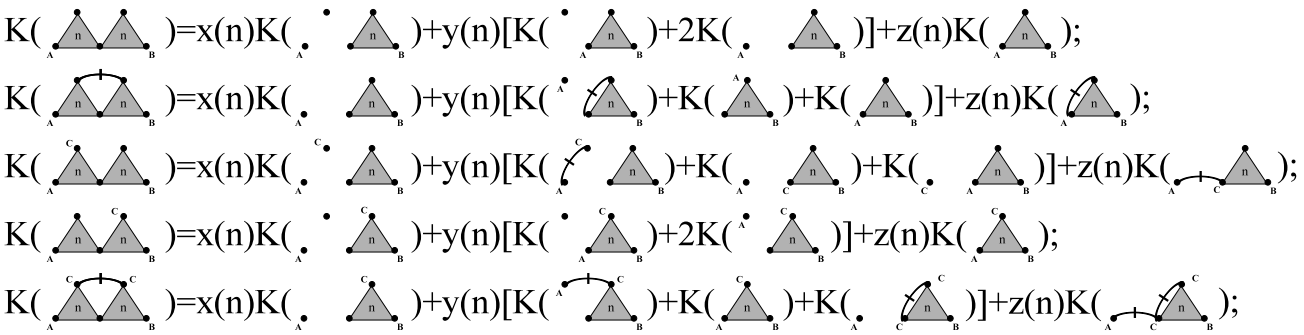

Figure 4: Decomposition of the five terms displayed in Fig.3.

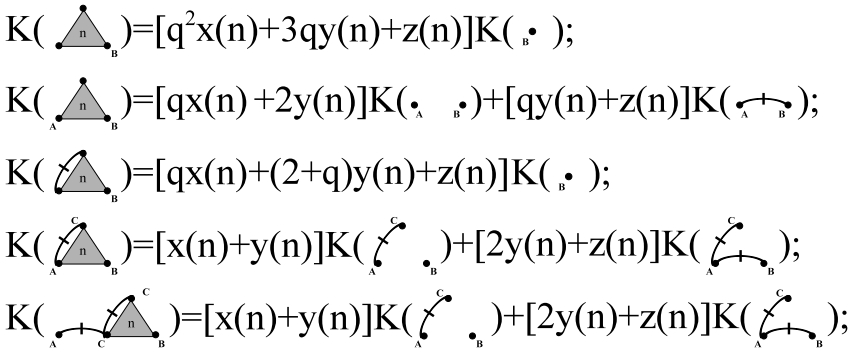

Figure 5: Decompositions of all the different types of terms appearing in Fig.4.

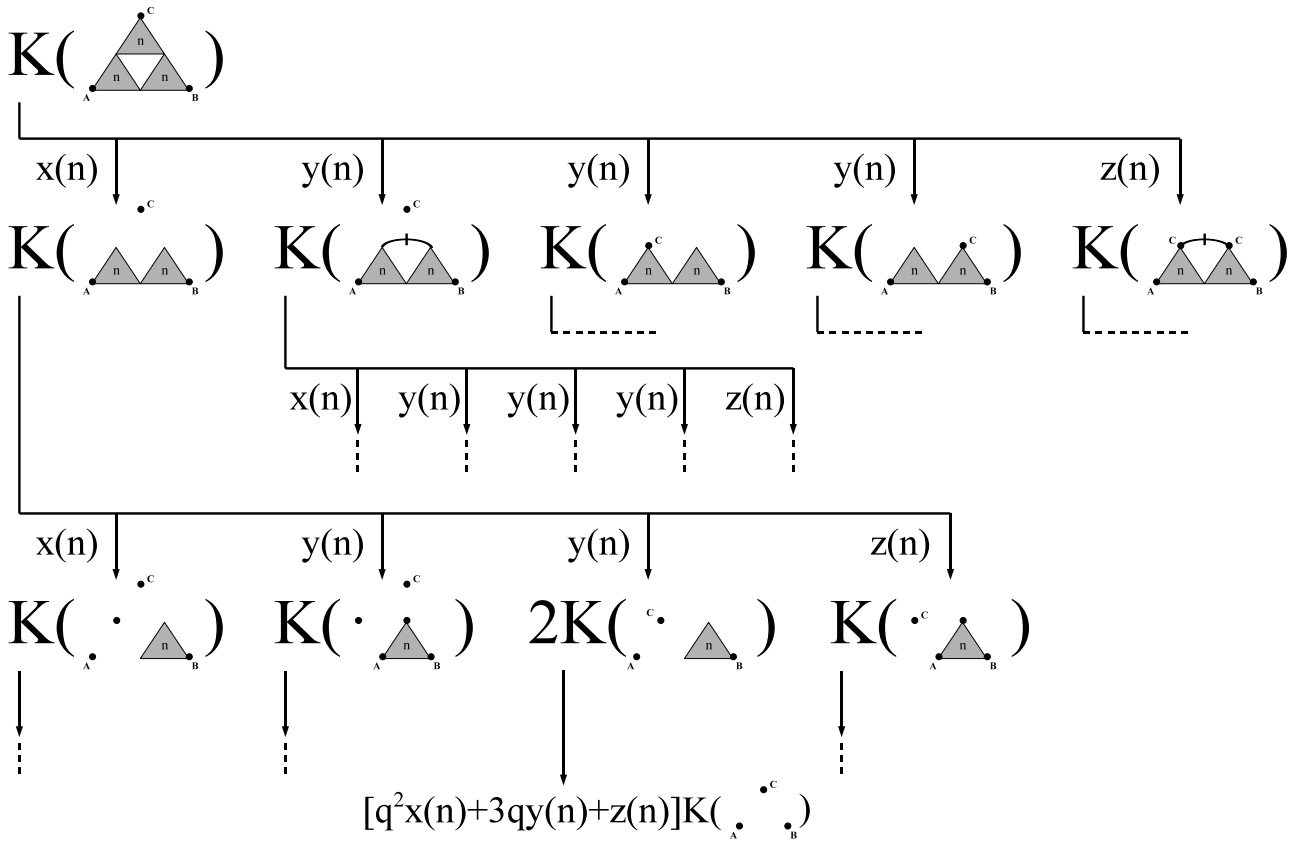

Figure 6: Scheme of the decomposition tree. Along any single path of decomposition indicated by an arrow, one has to keep track of the corresponding factor. In the picture, a specific path is followed up to the last step of the decomposition: $x(n)$ (first step) $y(n)$ (second step). It contributes to the coefficients $x(n+1)$ with a term $x(n)y(n)[q^2x(n)+3qy(n)+z(n)]$.

In this framework, the discrete evolution parameter n of the dynamical system (which is the recursive label of the Sierpinski triangles $T(n)$) corresponds to the size of the Sierpinski gasket $T(n)$. Hence, the thermodynamical limit corresponds to the asymptotic analysis of the dynamical system in Eqs. (4.1) together with the initial data in Eq. (4.2) when $n \to \infty$. It is also worth noting that, the temperature does not enter directly the dynamical system: in the present scheme, the dependence on the temperature (through v) only appears in the initial data in Eq. (4.2). On the other hand, the parameter q of the Potts model enters directly the equations of the dynamical system i.e. Eqs. (4.3), (4.4) and (4.5). The analysis can be performed for various interesting values of q; in the present paper we will focus on $q = 1.1$, $q = 1.5$ and $q = 2$. As it is well known in the theory of dynamical systems, the asymptotic behaviour is dominated by the attractive fixed points. In order to analyse the different phases of the Potts model on the Sierpinski triangle, one has to consider all the physically interesting ranges of v and then one has to study the corresponding evolutions of the dynamical system in Eqs. (4.1) for very large n.

The most evident gain of the present procedure can be seen as follows. If one would compute by "brute force" the partition function of the Potts model on the Sierpinski gasket after n steps, one should compute[5] 2^{n_l} terms using the definitions in Eqs. (2.2), (2.3) and (2.4). Therefore, roughly speaking, one should compute 2^{3^n} terms after n steps. On the other hand, if one uses Eqs. (2.2), (2.3) and (2.4) together with the initial data in Eq. (4.2), in order to get the partition function of the $n-$th step Sierpinski lattice one has to perform just $3n$ algebraic operations.

It is convenient to exploit the homogeneity of the polynomials in Eqs. (4.3), (4.4) and (4.5) in order to reduce the above dynamical system to a system of two equations in two variables, $\eta(n)$ and $\gamma(n)$, as follows:

$$\eta(n) = \frac{y\,(n)}{x\,(n)}, \qquad \gamma(n) = \frac{z\,(n)}{x\,(n)}, \tag{4.6}$$

[5] n_l is the number of edges of the $n-$step Sierpinski triangle.

so that one gets a closed system for η and γ:

$$\eta(n+1) = \frac{g(1,\eta(n),\gamma(n);q)}{f(1,\eta(n),\gamma(n);q)}, \qquad \gamma(n+1) = \frac{h(1,\eta(n),\gamma(n);q)}{f(1,\eta(n),\gamma(n);q)} \tag{4.7}$$

$$\eta(1) = v, \qquad \gamma(1) = v^2\,(3+v)\,. \tag{4.8}$$

The formulation of the dynamical system in Eqs.(4.7) is also convenient as far as the physical interpretation is concerned since the high temperature phase corresponds to the range of temperatures for which, in the large n limit,

$$|\eta(n)| \underset{n\to\infty}{\ll} 1, \qquad |\gamma(n)| \underset{n\to\infty}{\ll} 1,$$

while, in the antiferromagnetic phase, frustration at macroscopic scales appears if

$$|\eta(n)| \underset{n\to\infty}{\gtrapprox} O(1), \qquad |\gamma(n)| \underset{n\to\infty}{\gtrapprox} O(1).$$

(see the discussion below Eqs.(3.5) and (3.6)). Indeed, from the physical point of view, one is interested in the thermodynamical large n limit of the Sierpinski gasket partition function $K(n)$. Within the present framework, this corresponds to analyse the aymptotic behaviour of the dynamical system in Eqs. (4.7) in the large n limit for initial data of the form in Eq. (4.8) where v takes values both in the antiferromagnetic and in the ferromagnetic ranges.

In the section 6 we will show how to modify the initial data, corresponding to the Eq. (4.8) in order to consider different geometries of $T(1)$.

4.1 Fixed points of the Sierpinski Gasket's dynamical system

Here, we will discuss the properties of the fixed points of the Sierpinski Gasket's dynamical system. The dynamical evolution will be analyzed in more details in the next sections.

The system in Eqs. (4.7) admits ten fixed points which, in general, depend on the parameter q only. Except for the stationary points henceforth named P_1, P_2 and P_3, whose coordinates are $(\eta = 0, \gamma = 0)$, $(\eta = -\frac{1}{2}q, \gamma = \frac{1}{2}q^2)$ and $(\eta = -\frac{1}{2}q, \gamma = \frac{1}{4}q^2)$ respectively, the analytical expressions of the fixed points are rather cumbersome and not illuminating. Furthermore, the points P_1, P_2 and P_3 are the most important in our analysis since, as it will be shown in the next sections, they are the only relevant points as far as the evolution of the initial conditions is concerned.

The existence range and stability properties of the ten fixed points are summarized in Table 1 (see also Fig.10. It is worth noting a very peculiar feature of the present dynamical system. Even if the fixed point P_3 is unstable, it is relevant as far as the dynamics of the Sierpinski dynamical system is concerned: the technical reason is that such fixed points lies on the boundary of its own basin of attraction. This is a quite interesting feature as far as the theory of dynamical system is concerned.

Point	Allowed values of q	Stability
P1	$0 < q < \infty$	stable
P2	$0 < q < \infty$	stable
P3	$0 < q < \infty$	non-hyperbolic
P4	$0.815 < q < \infty$	unstable
P5	$0 < q < 2$	unstable
P6	$0.815 < q < 2$	unstable
P7	$0 < q < \infty$	unstable
P8	$0 < q < \infty$	unstable
P9	$3 < q < 7$ and $7 < q < \infty$	unstable
P10	$3 < q < \infty$	unstable

Table 1: Existence and stability of fixed points in the range $0 < q < \infty$. These results are obtained from both analytical results and numerical integrations.

5 Potts model on Hanoi graph

In this section the previous method to analyse the phase diagram of the Potts model on Sierpinski lattice will be applied to another interesting class of triangular self-similar lattices known in the literature as Hanoi graph (see Fig.7). Hanoi graph is defined recursively: this class of lattices will be denoted as $T_h(n)$ while, as in the previous sections, the three marked points (or vertices) of $T_h(n)$ will be denoted as $\bullet_a$, $\bullet_b$ and $\bullet_c$. The geometrical structure of the recursive transformation from the step n to the step $n+1$ is quite similar to the one of the Sierpinski lattice but there is an important difference: the lattice $T_h(n+1)$ can be see as three lattices $T_h(n)$ glued in such a way that the three triangles $T_h(n)$ constituting $T_h(n+1)$ are pairwise joined to each other trough an edge. We will consider the three edges which are pairwise shared by the three $T_h(n)$ blocks at step $n+1$ as *bold edges*: namely, in the following analysis, each of these three bold edges will be m simple edges in series of m' simple edges in parallel (where m and m' are positive integer numbers).

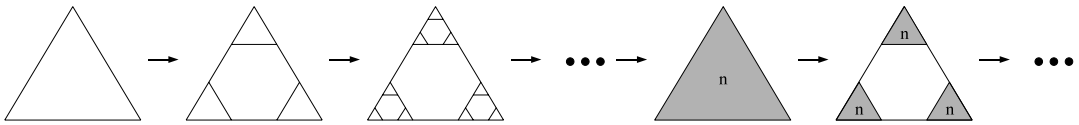

Figure 7: According with the recursive definition of the Hanoi graph, the three n-blocks at step $n+1$ are pairwise joined through edges.

Following the general procedure explained in sections 3 and 4, we expand the partition function of $T_h(n)$ in terms of the connectivity coefficients as follows,

$$\begin{aligned} K_h(n) = K[T_h(n)] &= x(n)\, K[\bullet_a\ \bullet_b\ \bullet_c] + z(n)\, K[\bullet_a = \bullet_b = \bullet_c] + \\ &\quad + y(n)\left\{K[\bullet_a = \bullet_b\ \bullet_c] + K[\bullet_a = \bullet_c\ \bullet_b] + K[\bullet_c = \bullet_b\ \bullet_a]\right\}. \end{aligned} \tag{5.1}$$

This definition allows one to express the connection coefficients $x(n+1)$, $y(n+1)$ and $z(n+1)$ of $T_h(n+1)$ in terms of the coefficients $x(n)$, $y(n)$ and $z(n)$ of the step n along the same line used to analyze the Sierpinski gasket. The resulting discrete dynamical system is

$$x(n+1) = f_h(x(n), y(n), z(n); q, v), \qquad y(n+1) = g_h(x(n), y(n), z(n); q, v), \qquad z(n+1) = h_h(x(n), y(n), z(n); q, v), \tag{5.2}$$

the corresponding initial data is given by

$$x(1) = 1, \qquad y(1) = v, \qquad z(1) = v^2(3+v). \tag{5.3}$$

The functions f_h, g_h and h_h are homogeneous polynomials of degree 3 and, in contrast with the ones for the Sierpinsky lattice, they include explicit dependence on the temperature, their explicit expressions being

$$\begin{aligned} f_h(x,y,z;q,v) &= \left(\frac{K_h(x,y,z;q)}{q}\right)^3 + 3v\frac{K_h(x,y,z;q)P(x,y;q)}{q}\left(\frac{K_h(x,y,z;q)}{q} + Q(y,z;q)\right) + \\ &\quad 3v^2\left((Q(y,z;q))^2 x + (P(x,y;q))^2\left(\frac{K_h(x,y,z;q)}{q} + 2Q(y,z;q)\right)\right) + v^3 f(x,y,z;q), \end{aligned} \tag{5.4}$$

$$g_h(x,y,z;q,v) = v\frac{K_h(x,y,z;q)\,(Q(y,z;q))^2}{q} + v^2\,(Q(y,z;q))^2\,(3y + 2P(x,y;q)) + v^3 g(x,y,z;q), \tag{5.5}$$

$$h_h(x,y,z;q,v) = 3v^2 z\,(Q(y,z;q,v))^2 + v^3 h(x,y,z;q). \tag{5.6}$$

The functions $f(x,y,z;q)$, $g(x,y,z;q)$ and $h(x,y,z;q)$ on the right hand side of Eqs. (5.4), (5.5) and (5.6) are defined in Eqs. (4.3), (4.4) and (4.5), $K_h(x,y,z;q)$ is defined in Eq. (5.1) and the following functions have been introduced:

$$P(x,y;q) = qx + 2y, \qquad Q(y,z;q) = qy + z.$$

It is worth to note here that in all the equations of the system there is a term which is the same as the corresponding term of the dynamical system in Eqs. (4.1) of the Sierpinski gasket multiplied by v^3.

Besides the terms which are similar to the corresponding terms of the Sierpinski gasket, in Eq. (5.4) for $x(n+1)$ there are three further terms. One term corresponds to the case in which all the three (bold) edges of $T_h(n+1)$ have

been deleted. Another term is proportional to v and corresponds to the case in which two (bold) edges of $T_h(n+1)$ have been deleted while one has been contracted. The last new term is proportional to v^2 and corresponds to the case in which two (bold) edges of $T_h(n+1)$ have been contracted while one has been deleted.

In Eq. (5.5) for $y(n+1)$ there are two new terms. One term is proportional to v and corresponds to the case in which two (bold) edges of $T_h(n+1)$ have been deleted while one has been contracted. The last new term is proportional to v^2 and corresponds to the case in which two (bold) edges of $T_h(n+1)$ have been contracted while one has been deleted.

In Eq. (5.6) for $z(n+1)$ there is only one new term: it is proportional to v^2 and corresponds to the case in which two (bold) edges of $T_h(n+1)$ have been contracted while one has been deleted.

Again, the discrete evolution parameter n of the dynamical system corresponds to the size of the Hanoi graph itself. Hence, the thermodynamical limit corresponds to the asymptotic analysis of the dynamical system in Eqs. (5.2) together with the initial data in Eq. (5.3) when $n \to \infty$. In order to analyse the different phases of the Potts model on the Hanoi graph, one has to study the corresponding evolutions of the dynamical system in Eqs. (5.2) for very large n.

It is useful to exploit the fact that the right hand sides of Eqs. (5.2) are homogeneous functions of degree 3 in order to reduce the dynamical system to a system of two equations in two variables. Thus, we take as basic variables $\eta = y/x$ and $\gamma = z/x$:

$$\eta(n+1) = \frac{g_h(1,\eta(n),\gamma(n);q,v)}{f_h(1,\eta(n),\gamma(n);q,v)}, \qquad \gamma(n+1) = \frac{h_h(1,\eta(n),\gamma(n);q,v)}{f_h(1,\eta(n),\gamma(n);q,v)}. \tag{5.7}$$

The initial data corresponding to a simple triangle are[6]

$$\eta(1) = v, \qquad \gamma(1) = v^2\,(3+v)\,. \tag{5.8}$$

The formulation of the dynamical system in Eqs. (5.7) is also convenient as far as the physical interpretation is concerned since, as it has been already discussed (see the discussion below Eqs. (3.5) and (3.6)), the high temperature phase corresponds to the range of temperatures for which, in the large n limit,

$$|\eta(n)| \underset{n\to\infty}{\ll} 1, \qquad |\gamma(n)| \underset{n\to\infty}{\ll} 1,$$

while, in the antiferromagnetic phase, frustration at macroscopic scales appears if

$$|\eta(n)| \underset{n\to\infty}{\gtrapprox} O(1), \qquad |\gamma(n)| \underset{n\to\infty}{\gtrapprox} O(1).$$

Indeed, from the physical point of view, one is interested in the thermodynamical large n limit of the Potts model partition function on the Hanoi graph $K_h(n)$. Within the present framework, this corresponds to analyse the asymptotic behaviour of the dynamical system in Eqs. (5.7) in the large n limit for initial data of the form in Eq. (5.8) where v takes values both in the antiferromagnetic and in the ferromagnetic ranges.

On the other hand, one can also consider the initial data in Eqs. (6.3), (6.4) and (6.6).

6 Changing lattices and initial data

In this section, we will analyze the physical meaning of changing the initial data of both the dynamical system in Eqs. (4.1) and of the dynamical system in Eqs. (5.2). Let us consider a class of lattices which will be denoted as $\widetilde{T}(n)$ where the label n denotes the recursive step. They can be defined recursively as follows. $\widetilde{T}(1)$ is a lattice with three marked points (denoted as $\bullet_a$, $\bullet_b$ and $\bullet_c$) and with triangular symmetry: namely, it is symmetric under a $2\pi/3-$rotation in the plane. There are two possibilities to proceed. Following the Sierpinski self-similar structure, $\widetilde{T}(2)$ can be obtained considering three $\widetilde{T}(1)$ blocks which pairwise share one marked point and so on (see, for instance, the example in Fig.8 (a)). Otherwise, following the Hanoi self-similar structure, $\widetilde{T}(2)$ can be obtained considering three $\widetilde{T}(1)$ blocks which pairwise share one edge and so on (see, for instance, the example in Fig.8 (b)). In both cases, the self-similar structure is the same as in the case of the Sierpinski gasket and Hanoi graph respectively but the "starting point" (namely, the first lattice $\widetilde{T}(1)$) can be quite different. Indeed, the thermodynamical properties, such as the critical temperature indicating the arising of macroscopic frustration, are quite sensitive to the choice of the "starting point".

[6]It is also possible to consider different initial data corresponding to a different choice of $T(1)$ as it will be explained in the next section.

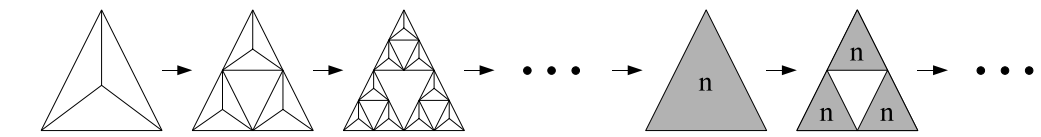

(a)

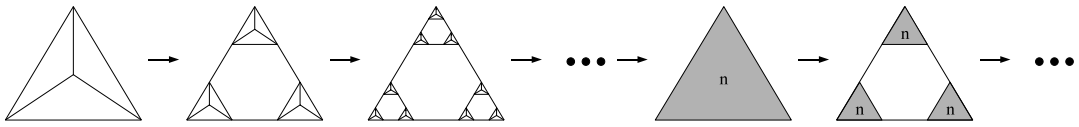

(b)

Figure 8: (a) The recursive step between the steps n and $n+1$ is the same as in the Sierpinski gasket, therefore the dynamical system for this lattice is the same as that of Sierpinski but with different initial conditions. (b) The recursive relation between the steps n and $n+1$ is the same as in the Hanoi graph, therefore the dynamical system for this lattice is the same as that of Hanoi but with *Borromean*[7] initial data.

It is very interesting to explore how the thermodynamical properties change according to the change of $\widetilde{T}(1)$. This task is made possible by the following observation: even if, when $\widetilde{T}(1)$ is not a simple triangle and so the lattices one obtains are neither the Sierpinski gasket nor the Hanoi graph, the dynamical systems which describe the thermodynamical properties of the Potts model on the lattices described above is exactly the same as in the Sierpinski case or in the Hanoi case. The reason is that in order to derive the dynamical system one has to define the connectivity coefficients at step n (see Eq. (3.1)) and then compare the step n with the step $n+1$ and, to do this, one does not need any information about $\widetilde{T}(1)$ (besides, of course, its triangular symmetry). Therefore one can still use the dynamical systems in Eqs. (4.1), as well as the Hanoi dynamical system in Eqs. (5.2) (or, even better, the reduced versions in Eqs. (4.7) for Sierpinski and in Eqs. (5.7) for Hanoi). The difference is just in the initial data which are in one-to-one correspondence with the "starting points" $\widetilde{T}(1)$. This remark provides one with a very simple way to construct systems with multiple phase transitions as it will be shown in the next section.

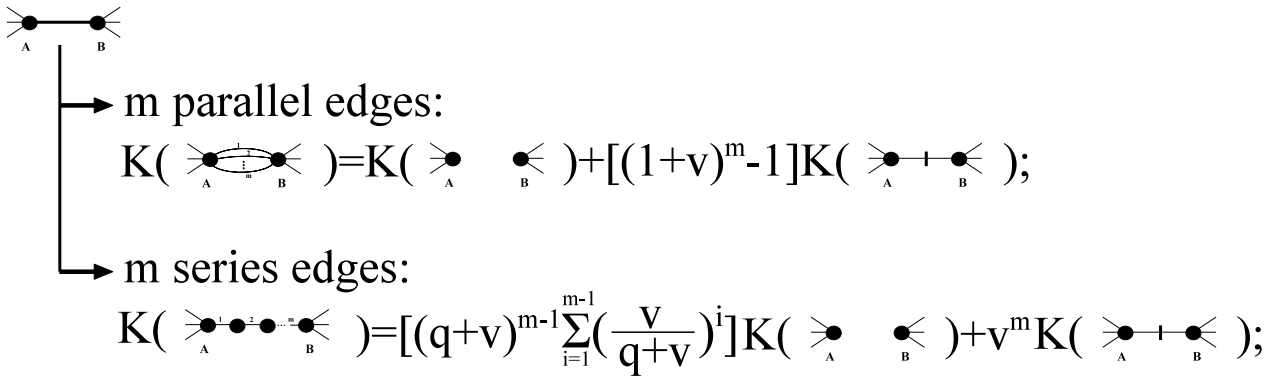

Figure 9: Two types of bold edges are depicted, namely m simple edges either in series or in parallel. The deletion of m parallel edges connecting two marked vertices ($\bullet_A$ and $\bullet_B$) gives rise to a factor 1 while the contraction to gives rise to a factor $(1+v)^m - 1$. Likewise, the deletion of m edges in series between two marked vertices gives rise to a factor $(q+v)^{m-1}\sum_{1=0}^{m-1}\left(\frac{v}{q+v}\right)^i$ while the contraction gives rise to a factor v^m.

[7]This name is due to the fact that this graph is dual to the Borromean link in the sense of the relation between graphs and knots (see, for instance [30, 31, 32]).

6.1 Examples

Before analyzing the more interesting case of multiple phase transitions, here we will consider lattices in which all the edges are replaced by m edges in series or m' edges in parallel (m and m' being positive integer numbers greater than one) in such a way to respect the triangular symmetry (see Fig.9): these structures will be denoted as *bold edges*. As initial block $\widetilde{T}(1)$ we will consider a triangular lattice with a vertex in the barycentre connected to the three marked points of $\widetilde{T}(1)$. $\widetilde{T}(1)$ has two types of (bold) edges: the external (bold) edges which connect the marked points between themselves and the internal (bold) edges which connect one marked point with the barycentre of the $\widetilde{T}(1)$ (see Fig.9). Let us define the *bold edge* which connects two vertices (say $\bullet_a$ and $\bullet_b$) as the sub-lattice with two marked points such that the marked points coincide with the two vertices $\bullet_a$ and $\bullet_b$. We will consider here only the cases in which the bold edge is made up by m simple edges in series joining the two vertices $\bullet_a$ and $\bullet_b$ or m' simple edges in parallel joining the two vertices $\bullet_a$ and $\bullet_b$ (see Fig.9). Each of these two cases can be easily described in terms of two coefficients.

Using the defining rules of the dichromatic polynomial (i.e. Eqs. (2.2), (2.3) and (2.4)) in the case of m edges in series, the corresponding bold edge can be characterized by two coefficients $A_s^{(m)}$ and $B_s^{(m)}$

$$A_s^{(m)} = \frac{v}{q}\left((q+v)^{m-1} - v^{m-1}\right), \qquad B_s^{(m)} = v^m. \tag{6.1}$$

The coefficient $A_s^{(m)}$ corresponds to the deletion of the bold edge (after which the two vertices as $\bullet_a$ and $\bullet_b$ are separated). The coefficient $B_s^{(m)}$ corresponds to the contraction of the bold edge (after which the two vertices as $\bullet_a$ and $\bullet_b$ are contracted).

On the other hand, using the defining rules of the dichromatic polynomial in the case of m' edges in parallel connecting the two vertices $\bullet_a$ and $\bullet_b$, the bold edge can be characterized by two coefficients $A_p^{(m')}$ and $B_p^{(m')}$

$$A_p^{(m')} = 1, \qquad B_p^{(m')} = (1+v)^{m'} - 1. \tag{6.2}$$

The coefficient $A_p^{(m')}$ corresponds to the deletion of the bold edge (after which the two vertices as $\bullet_a$ and $\bullet_b$ are separated). The coefficient $B_p^{(m')}$ corresponds to the contraction of the bold edge (after which the two vertices as $\bullet_a$ and $\bullet_b$ are contracted).

It can be easily checked that the new initial data can be written as follows:

$$\eta(1) = \frac{y(1)}{x(1)}, \qquad \gamma(1) = \frac{z(1)}{x(1)}, \tag{6.3}$$

where

$$x(1) = (3v_{int} + q\delta_{int})(\delta_{int})^2(\delta_{ext})^3, \tag{6.4}$$

$$y(1) = (3v_{int} + q\delta_{int})(\delta_{int})^2(\delta_{ext})^2 v_{ext} + \delta_{int}(v_{int})^2(\delta_{ext})^2(\delta_{ext} + v_{ext}), \tag{6.5}$$

$$z(1) = (3v_{int} + q\delta_{int})(\delta_{int})^2(3\delta_{ext} + v_{ext})(v_{ext})^2 + (v_{int})^3(\delta_{ext} + v_{ext})^3 + \\ +3\delta_{int}(v_{int})^2 v_{ext}(\delta_{ext} + v_{ext})(2\delta_{ext} + v_{ext}). \tag{6.6}$$

The coefficients (δ_{int}, v_{int}) characterize the internal bold edges which connect the marked points of $\widetilde{T}(1)$ with the vertex at the center of $\widetilde{T}(1)$ itself. Since the internal bold edges can be either in series orin parallel we have correspondingly two possibilites:

$$\delta_{int} = A_s^{(m)}, \qquad v_{int} = B_s^{(m)},$$

or

$$\delta_{int} = A_p^{(m')}, \qquad v_{int} = B_p^{(m')}.$$

In the same way, the coefficients (δ_{ext}, v_{ext}) characterize the external bold edges which connect the marked points of $\widetilde{T}(1)$ between themselves. Since the external bold edges can be either in series or in parallel we have correspondingly two possibilities:

$$\delta_{ext} = A_s^{(m)}, \qquad v_{ext} = B_s^{(m)},$$

or

$$\delta_{ext} = A_p^{(m')}, \qquad v_{ext} = B_p^{(m')}.$$

Thus, there are four possibilities depending on the choices of the internal and external bold edges as edges in series or parallel: below we will describe how the behaviour of the system changes accordingly. It appears that replacing

edges with edges in series or parallel does not introduce new features in the phase diagram of the systems. In the ferromagnetic phase, neither the Sierpinski dynamical system nor the Hanoi dynamical system display interesting phase diagrams. However, it is reasonable to expect that self-similar lattices with Hausdorff dimensions higher than the Sierpinski Hausdorff dimension (but still less than two) could have richer ferromagnetic phase diagrams. This issue is worth to be further investigated.

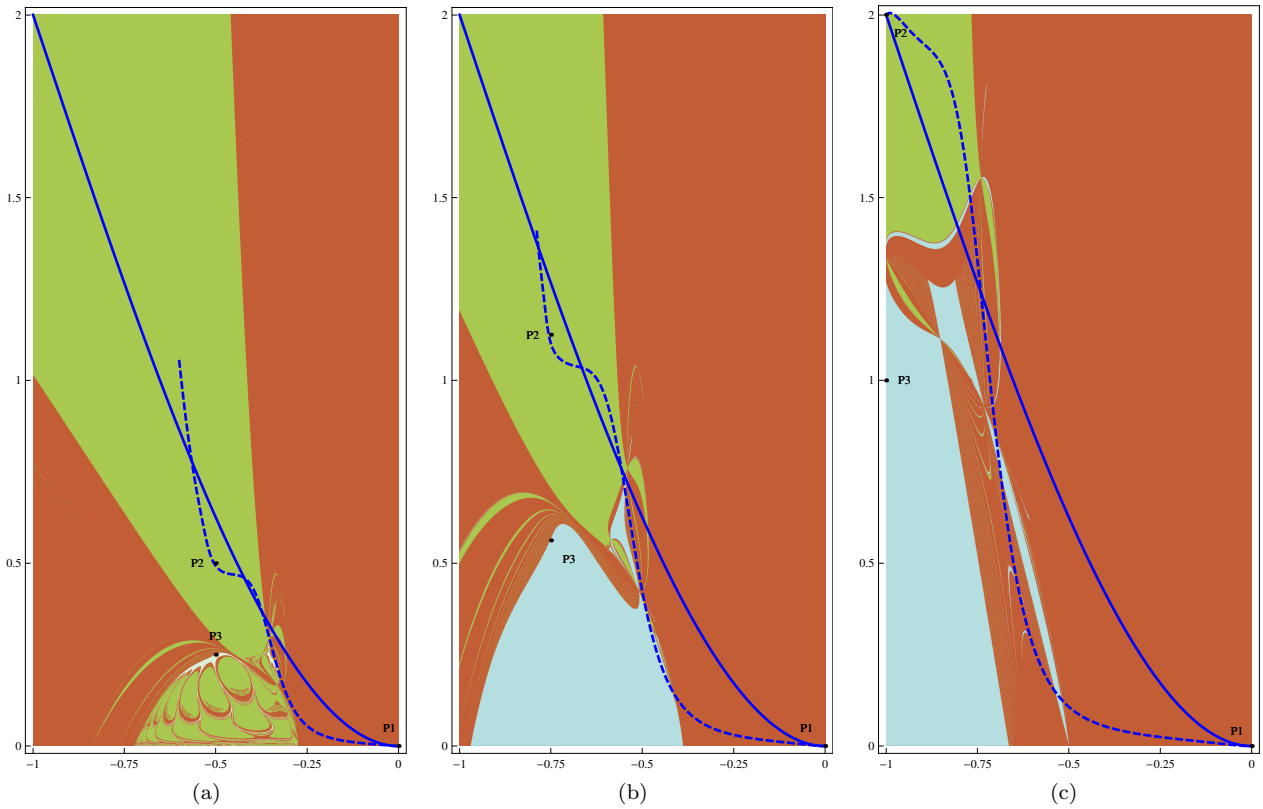

Figure 10: Basins of convergence of the Sierpinski map in the antiferromagnetic regime for (a) $q = 1$, (b) $q = 1.5$ and (c) $q = 2$. The behavior of two different initial data, standard triangle in continue line and the Hanoi of second step in dashed line is indicated. The brown color indicates the basin of P1, the green color indicates the basin of P2, and sky-blue indicates the basin of P3. When the lines of initial data cross over a zone of different color then there is a phase transition. Multiple phase transitions appear wherever the blue lines cross several times the boundary of different basins.

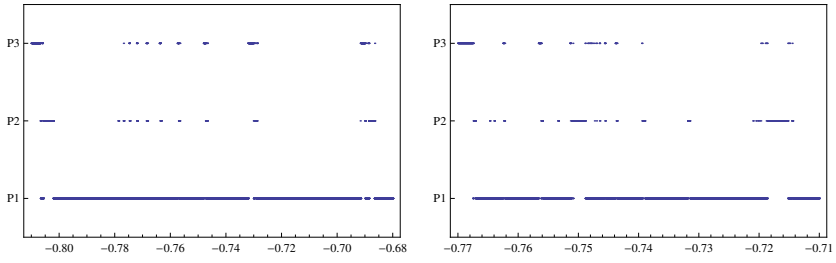

Figure 11: A zoom to the ranges of temperature where the multiple phase transitions occur is shown for the Sierpinski dynamical system with $q = 2$ for two different initial values: (a) Simple triangle and (b) the Hanoi of second step.

The clearest way to visualize the consequences of changing initial data is provided by the map of basins in the plane η-γ. The idea is to overlap the curves associated to the usual initial data (i.e. a triangle) or the 1-step Hanoi initial data and check how many times the curves cross the basins of the stable fixed points (see Fig. 10).

7 Multiple transitions

It will be now discussed how the previous construction can be used to generate self-similar lattices on which the Potts model manifests multiple phase transtions. In order for this to happen, one should find a suitable initial triangular lattice $\widetilde{T}(1)$ which generates initial data such that the corresponding curve in the η-γ plane crosses at least two boundaries between different basins of attraction. The different phases of the system correspond to different degrees of macroscopic frustration. In particular, the two non-trivial fixed points $(\eta = -\frac{1}{2}q, \gamma = \frac{1}{2}q^2)$ and $(\eta = -\frac{1}{2}q, \gamma = \frac{1}{4}q^2)$ represent different phases since the amount of frustration when the system is in the basins of the fixed point $(\eta = -\frac{1}{2}q, \gamma = \frac{1}{2}q^2)$ is bigger than the amount of frustration when the system is in the basins of the other non-trivial fixed point. Therefore, these multiple critical temperatures represent sudden jumps in the number of macroscopic frustrated paths connecting the vertices of the self-similar lattice.

In Fig.10 we have drawn the basins of convergence of the Sierpinski map in the antiferromagnetic regime for (a) $q = 1.1$, (b) $q = 1.5$ and (c) $q = 2$. The continuous and the dashed lines in Fig.10 represent the initial data corresponding to the simple triangle and to the Hanoi triangle respectively. Namely, the continuous line in Fig.10 corresponds to the initial data for the Sierpinski dynamical system of an initial triangular lattice $\widetilde{T}(1)$ which is a simple triangle (see Eq. (4.2)). On the other hand, the dashed line in Fig.10 corresponds to the initial data for the Sierpinski dynamical system of an initial triangular lattice $\widetilde{T}(1)$ which is a one-step Hanoi triangle. The most complex phase diagrams occurr when one get closer and closer to $q = 1$: of course, this limit is very interesting for the analysis of percolation. In particular, Fig.10 (a) shows a fractal structure of the basins of attraction in the case of $q = 1.1$ (see in particular the region below the fixed point P_3 in which there is a brown wavy like structure "propagating" inside the green region). This makes difficult to consider the $q \to 1^+$ limit and, in particular, to compute numerically derivatives with respect to q in that limit. This issue is worth to be further investigated.

7.1 Sierpinski dynamical system

The basin map of the Sierpinski dynamical system for $q = 2$ (Fig.10 (c)) shows the presence of various critical temperatures which correspond to the continuous line of initial data crossing different basins of attractions. It is apparent that, in the case of the dashed line of initial data (which represents the one-step Hanoi triangle as initial data for the Sierpinski dynamical system), the number of sudden crossings from one basin of attraction to another increases substantially. In Fig.11 we showed a zoom of the ranges of temperature where the multiple phase transitions occur, with $q = 2$, for two different initial data: (a) simple triangle and (b) one-step Hanoi. On the horizontal axis in Fig.11 there is the temperature variable v, while on the vertical axis there are three possible coordinates corresponding to the three possible fixed points. Thus, for instance, in Fig.11 a plateau at the level of the fixed point P_2 corresponds to a range of temperatures in which the relevant fixed point is P_2. The present method displays clearly the surprising complexity of the phase diagram corresponding to the Sierpinski dynamical system with many sudden jumps both for the triangle initial data and for the one-step Hanoi initial data.

7.2 Hanoi dynamical system

The previous examples are very interesting since to construct explicit examples of statistical systems with a simple enough Hamiltonian as well as with multiple critical temperatures is well known to be quite difficult (see, for instance, the discussion in [33]). In the case of the Hanoi graph, the equations of the corresponding dynamical system depend explicitly on the temperature variable v so that it is not possible to describe the evolution of the dynamical system itself using the basins map as in the Sierpinski case, as it has been done in Fig.10. Therefore, in the Hanoi case the dynamical evolution corresponding to Eqs. (5.7) with initial data in Eq. (5.8) will be represented, in Fig.12 with a map analogous to the one in Fig.11. It is interesting to note that, unlike the Sierpinski case, in the case of the Hanoi dynamical system with initial data in Eq. (5.8) there is just one critical temperature $v \sim -0.77$. An intuitive explanation for this is that one should expect that the complexity of the phase diagram increases as long as the Hausdorff dimension approaches to two. Therefore, it is a quite reasonable result that the phase diagram of the Potts model on the Sierpinski gasket is more complicated than the phase diagram corresponding to the Hanoi graph.

8 Conclusions

In the present paper, an analytic study of the Potts model partition function on self-similar triangular lattices has been presented. Two cases have been analyzed in details: the Sierpinski gasket and the Hanoi graph. The interest of both lattices lye in the fact that their Hausdorff dimensions are between one and two. This makes the corresponding

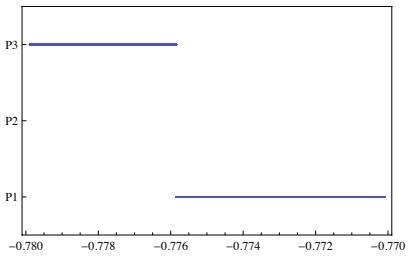

Figure 12: A zoom to the range of temperature where the phase transition occurs for the Hanoi dynamical system with $q = 2$.

thermodynamics very interesting theoretical arenas for the analysis of critical phenomena. The Potts model on the Sierpinski lattice has been analyzed using the formalism of the dichromatic polynomial. By introducing suitable geometric coefficients related to the connectivity pattern of the vertices of the Sierpinski gasket it is possible to reduce the computation of the partition function to a dynamical system. Then, using known results in the theory of dynamical systems, one can determine the possible phases of the system by analyzing the fixed points of the dynamical system itself. The same approach has been followed in the analysis of the Hanoi graph. Eventually, it has been shown that the formalism can be easily extended to other families of recursive lattices and initial conditions. The main advantage of the present method is that it allows to easily construct self-similar lattices with multiple critical temperatures which represent sudden jumps in the amount of frustration of the system. The problem is reduced to find suitable initial data for the dynamical systems corresponding to the Sierpinski gasket (the Hanoi graph has a less complex phase diagram, at least in the case of simple initial data) which cross more than once the boundary between two basins of attraction of the fixed points of the corresponding dynamical system. Therefore, self-similar lattices can give rise to a surprisingly complex phase diagrams.

Acknowledgements

This work has been partially funded by the following Fondecyt grants: 11080056, 3100140, and by the Conicyt grant "Southern Theoretical Physics Laboratory" ACT-91. The Centro de Estudios Cient´ıficos (CECS) is funded by the Chilean Government through the Centers of Excellence Base Financing Program of Conicyt. CIN is funded by Conicyt and the Gobierno Regional de Los R´ıos. The work of F. C. and L.P. has been partially supported by Agenzia Spaziale Italiana (ASI), and by the Italian Ministero Istruzione Università e Ricerca (MIUR) through the PRIN 2008 grant; F. C. has been partially supported also by PROYECTO INSERCION CONICYT 79090034.

References

[1] J. Zinn-Justin, *Quantum Field Theory and Critical Phenomena,* Oxford University press, (2002).

[2] R. J. Baxter, *Exactly Solved Models in Statistical Mechanics*, Dover Publications (New York), edition 2007.

[3] S. H. Strogatz, *Nonlinear dynamics and chaos: with applications to physics, biology, chemistry, and engineering*, Westview Press (1994).

[4] J. Wainwright, G.F.R. Ellis *Dynamical Systems in Cosmology*, Cambridge University Press, (1997).

[5] F. Y. Wu, *Rev. of Mod. Phys.* **54**, (1982) 235.

[6] C. N. Yang and M. L. Ge editors, *Braid group, knot theory and statistical mechanics II*, Advanced Series in Mathematical Physics Vol. 17, World Scientific (1994).

[7] J. Cardy, "*Conformal Invariance and Percolation*", arXiv:math-ph/0103018.

[8] B. Svetitsky, L. G. Yaffe, *Nucl. Phys. B* **210**, (1982) 235.

[9] L. Onsager, *Phys. Rev.* **65** (1944), 117.

[10] J. Salas, A. D. Sokal, "*Transfer matrices and partition-function zeros for antiferromagnetic Potts models. VI. Square lattice with special boundary conditions*", arXiv:1002.3761.

[11] S. Chang, R. Shrock, *PHYSICA A* **364** (2006), 231.

[12] S. Chang, R. Shrock, *J. Stat. Phys.* **130** (2008), 1011.

[13] D. Dhar, *J. Math. Phys.* **18**, (1977) 577.

[14] D. Dhar, *J. Math. Phys.* **19**, (1978) 5.

[15] D. Andelman, A. N. Berker, *J. Phys. A: Math. Gen.* **14**, (1981) L91-L96.

[16] R. B. Griffiths, M. Kauffman, *Phys. Rev. B* **26**, (1982) 5022-5032.

[17] M. Kauffman, R. B. Griffiths, *Phys. Rev. B* **30**, (1984) 244-249.

[18] Y. Gefen , A. Aharony, Y. Shapir and B.B. Mandelbrot, *J. Phys. A: Math. Gen.* **17**, (1984) 435-44.

[19] M. de Oliveira, S. Salinas, *Phys. Rev. B* **35**, (1987) 8744-8746.

[20] Z. Borjan, M. Knezevic, S. Milosevic, *Phys. Rev. B* **47**, (1993) 144.

[21] F. S. de Menezes and A. C. N. de Magalhães, *Phys. Rev. B* **46**, (1992) 11642-11656.

[22] A. Chame and U. M. S. Costa, *J. Phys. A: Math. Gen.* **23**, (1990) L1127.

[23] C. N. de Magalhães, S. R. Salinas and C. Tsallis *J. Phys. A: Math. Gen.* **31**, (1998) L567.

[24] P. T. Muzy nad S. R. Salinas, *IJMPB* **13**, (1999) 397-409.

[25] P. T. Muzy, A. P. Vieira, S. Salinas, *Phys. Rev. E* **65**, (2002) 046120.

[26] J. De Simoi, *Journ. Phys. A* **42**, (2009) 095002.

[27] F. Canfora, L. Parisi, G. Vilasi, *Phys. Lett. B* **638,** (2006) 85;
F. Canfora, *Phys. Lett. B.* **646**, (2007) 54;
M. Astorino, F. Canfora, C. Martinez, L. Parisi, *Phys. Lett. B* **664**, (2008) 139;
M. Astorino, F. Canfora, G. Giribet, *Phys. Lett. B* **671**, (2009) 291;
M. Astorino, F. Canfora, *Phys. Rev. E* **81**, (2010) 051140.

[28] P. Alvarez, F. Canfora, S. Reyes, S. Riquelme, *"Potts model on recursive lattices: some new exact results"*, arXiv:0912.4705

[29] N. L. Biggs, R. M. Damerell, and D. A. Sands, *J. Combin. Theory B* **12**, (1972) 123-131;
S. Beraha and J. Kahane,*J.Combin. Theory B* **27**, (1979) 1-12;
S. Beraha, J. Kahane and N. J. Weiss, *J. Combin. Theory B* **28**, (1980) 56-65.

[30] L.H. Kauffman, *Trans. Amer. Math. Soc.* **318**, (1990) 417–471.

[31] L.H. Kauffman, *Knots and Physics*, World Scientific, (2001).

[32] F. Y. Wu, *Rev.of Mod. Phys.* **64**, (1992) 1099.

[33] J. B. Kogut, *Rev. Mod. Phys.* **51**, 659 (1979).